J Mater Sci (2008) 43:602–608
DOI 10.1007/s10853-007-1743-2

5TH BRAZILIAN MRS MEETING

Effect of scandium on the structural and photocatalytic properties of titanium dioxide thin films

A. A. Cavalheiro · J. C. Bruno · M. J. Saeki · J. P. S. Valente · A. O. Florentino

Received: 18 December 2006 / Accepted: 3 April 2007 / Published online: 22 June 2007

Abstract Pure and scandium doped-TiO_2 thin films were prepared by the sol-gel process and coated by dip coating. The effects of scandium on the phase formation, optical properties and photoactivity of the TiO_2 thin films were investigated. The lattice parameters and the crystallinity of the anatase phase, characterized by the Rietveld method, demonstrated that scandium doping affected the structural parameters and crystallinity of the films, modifying the absorption edge. A direct correlation was found between band gap energy and photodegradation efficiency, with lower values of band gap energy augmenting this efficiency. Moreover, a significant improvement in the catalyst's photodegradation efficiency was attained with a scandium concentration of 5.0 mol%.

Introduction

Titanium dioxide is the photocatalyst most widely used in environmental purification, applied in the degradation of organic pollutants and in self-cleaning production processes [1–3]. Since of their biological properties and bioaccumulating effect, pharmaceutical substances are an example of pollutants that can impact the environment. Diclofenac potassium is a nonbiodegradable antiinflammatory drug which is present in high concentrations in treated effluents and rivers around the world. Though not a dangerous compound, the high level of contamination resulting from its intensive use and from the photochemical degradation of its by-products make it one of the most serious contaminants [4, 5].

Much attention has focused on the photocatalytic activity of TiO_2 semiconductors under supra-bandgap ultraviolet illumination. When TiO_2 absorbs UV rays at <380 nm, the electron is excited from valence to the conduction band, and the positive hole from which the electron emerged is generated inside the TiO_2 [6]. The photogenerated electron–hole pairs can react with species at the surface to produce highly oxidizing species capable of mineralizing organics adsorbed on the TiO_2 surface [7]. In aqueous media, photogenerated electrons interact with oxygen dissolved in water or with organic molecules to produce radicals, while the holes can oxidize organic molecules directly or interact with water molecules to produce hydroxyl groups [8].

In the photocatalytic reaction of TiO_2, the use of sunlight or visible light as source of irradiation is limited, which is why new attempts have been made to improve this material [6]. In addition, the influence of the synthesis parameters on the physical properties of TiO_2 thin films, mainly in terms of the crystal structure and crystallite size, which are important factors in the performance of photocatalytic activity, has not been sufficiently investigated so far. For instance, only a few reports describe the photocatalytic activity of low crystallized TiO_2 [9–11].

An important goal in the development of such a photocatalyst, aiming to advance its practical application, is to modify the material by doping. The addition of foreign metal ions such as Fe^{3+}, Cu^{2+}, Ag^{+}, and Pt^{4+} affects the TiO_2 phase formation, structure and photocatalytic activity [12, 13]. Dopants can be inserted by the sol-gel method,

A. A. Cavalheiro (✉) · J. C. Bruno · M. J. Saeki · J. P. S. Valente · A. O. Florentino
Depto de Química, Instituto de Biociências, UNESP, Distrito de Rubião Junior, s/n, P.O. Box 510, 18618-000 Botucatu, SP, Brazil
e-mail: albecava@bol.com.br

which is a suitable method for preparing TiO_2 films. This process consists of the hydrolyzation of a titanium alkoxide followed by condensation and polymerization reactions. No high temperature is required to prepare the solution, which can be deposited on the substrate by different techniques such as dip or spin coating [14].

In this work, the sol-gel process and dip-coating technique were used to prepare scandium doped-TiO_2 thin films. The phase formation and the structural parameters were studied by X-ray diffraction and by the Rietveld method. The optical and morphological properties are also discussed, and the efficiency of the scandium doped-TiO_2 catalyst verified for the degradation of diclofenac potassium solution.

Experimental

Titanium isopropoxide (98%) and scandium oxide (99.9%) were used to prepare $Sc_xTi_{(1-x)}O_2$ thin films, where $x = 0$, 0.005, 0.02 and 0.05. The precursor solutions were prepared via the sol-gel method using a molar rate of 1:4 (titanium isopropoxide: acetic acid). After the addition of isopropylic alcohol, the solution was stirred for 30 min, and a given amount of water and nitric acid was added to it and mixed until a transparent sol was formed. To prepare the doped samples, the scandium nitrate precursor was added together with the nitric acid solution. The films were prepared by coating the final solution, with a viscosity of 20 cP, onto borosilicate glass substrate by dip coating. Applying a withdrawal speed of 0.3 mm and immersion time of 10 s, the film was coated three times and heat-treated at 250 °C for 15 min to eliminate humidity and volatile substances after each deposition. Upon completion of the coating process, the films were calcined at 450 °C for 4 h in a muffle-type furnace in a static atmosphere.

The phase formation was investigated using a Rigaku D/MAX-2100/PC X-ray diffraction spectrometer with Ni-filtered Cu Kα radiation. The scanning range was 20–80° (2θ) with a step size of 2° and a count time of 1 min. The data obtained were used to determine the variations in the crystal structure, using the Rietveld structural refinement method (DBWS-9807 program) [15–17]. The thin films were also characterized by UV–vis spectroscopy (Ultrospec 2000) in transmission mode, in the wavelength region of 300–1,000 nm. The film thickness was calculated from the UV–vis spectra, using the fringe counting program (FTG – Version 1.02d software). Scanning electron microscopy (SEM LEO-440 microscope) was used to characterized the films' morphology and corroborate the thickness data obtained with the FTG software. The photocatalytic activity of the films was evaluated based on the degradation of the diclofenac potassium ($C_{14}H_{10}Cl_2KNO_2$) solution (TOC 1.0 mg L^{-1}). The experiment was conducted at 28 °C, under constant stirring, a bubbling oxygen flow, UV-A light irradiance of 365 nm (4.7 mW cm^{-2}), and protected from external light. The solution was quantified according to total organic carbon (TOC) (SHIMADZU, TOC-VCPH analyzer).

Results and discussion

Figure 1 shows the X-ray diffraction pattern of nondoped and scandium-doped TiO_2 thin films. All the reflections correspond to the anatase phase (JCPDF: 21-1272), which is related with the structural model available in the ICSD data bank under card number 92-353. The data obtained by Rietveld refinement (Table 1) show a loss of crystallinity in the scandium-doped TiO_2 samples compared to pure TiO_2, indicated by an increase in the values of the full width at half maximum (FWHM) of the most intense peak at 25.3°.

The variations in the lattice parameters of the anatase structure are also shown in Table 1. The scandium doping process tends to cause an increase in the cell volume of the anatase phase because the ionic radius of Sc^{+3} (0.745 Å) is larger than that of Ti^{+4} (0.605 Å), considering the coordination number of VI for both cations [18]. However, this structural effect is strongly anisotropic and seems to be influenced by the amount of oxygen vacancies created by the heterovalent character of the dopant. At low dopant concentrations, the cell volume diminishes in response to the decrease in the *a* and *c* parameters, probably influenced mostly by the reduction of the oxygen vacancy annihilation rate. Probably, this occurs because the insertion of scandium into TiO_2 enhances the refractory character of TiO_2, damaging the ionic diffusion during the crystallization process. Thus, the FWHM values keep increasing up to 2.0 mol% of scandium ($Sc_{0.02}Ti_{0.98}O_2$ sample), remaining unaltered in the $Sc_{0.05}Ti_{0.95}O_2$ sample. At a scandium concentration of 2.0 mol%, the *c* parameter was higher than that of the $Sc_{0.005}Ti_{0.98}O_2$ sample, but lower than that of the pure sample. However, the cell volume of the $Sc_{0.02}Ti_{0.98}O_2$ sample was higher than that of the pure sample, since the *a* parameter of the TiO_2 anatase structure is more susceptible to enlargement when a large cation substitutes the titanium cation. With 5.0 mol% of Sc ($Sc_{0.05}Ti_{0.95}O_2$ sample), both the *a* and *c* parameters increased, making the cell volume significantly higher to that of the other samples, because this sample contained a high concentration of Sc^{+3} (large cation) in relation to the associated oxygen vacancies.

The increase observed in the R_B index values (Table 1) indicates a reduction of the congruence of the real structure with the structural model as a function of the scandium

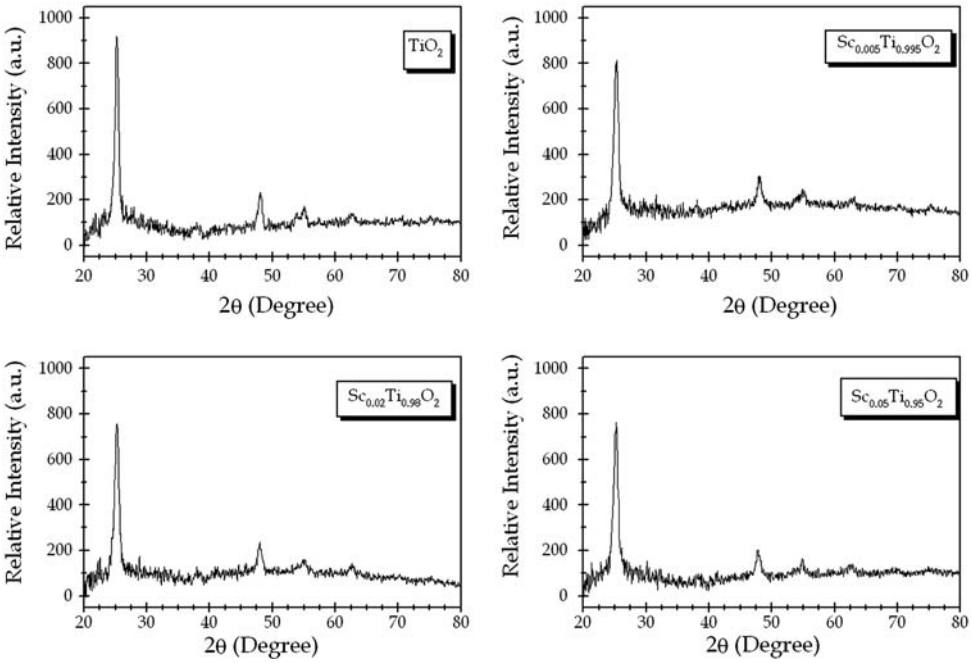

Fig. 1 XRD patterns of TiO_2, $Sc_{0.005}Ti_{0.995}O_2$, $Sc_{0.02}Ti_{0.98}O_2$ and $Sc_{0.05}Ti_{0.95}O_2$ thin films

Table 1 Structural parameters for the TiO_2 films obtained by Rietveld structural refinement

Sample	R_{WP}	S	R_B	a (Å)	c (Å)	V (Å^3)	FWHM
TiO_2	4.00	1.13	13.26	3.7890	9.5219	136.70	0.640
$Sc_{0.005}Ti_{0.995}O_2$	4.01	1.14	15.68	3.7853	9.4727	135.73	0.740
$Sc_{0.02}Ti_{0.98}O_2$	4.07	1.14	18.28	3.7952	9.5062	136.92	0.760
$Sc_{0.05}Ti_{0.95}O_2$	4.08	1.13	19.70	3.8088	9.5610	138.70	0.760

concentration. The value of the R_B index was not sufficiently small even for the pure sample, since low crystallinity is associated with the level of atomic order. The low values of the R_{wp} index, which refers to the adjustment of the calculated and observed data, show a good quality of refinement, and the goodness of fit (S index) of all the refined samples confirms that excellent results were achieved, indicating the high accuracy of these results. The S index is the R_{wp}/R_{exp} ratio, where R_{exp} is the statically possible maximum value for R_{wp}, considering the quality of the acquired data and the number of refined parameters.

Considering the optical properties of the thin films and the effects of scandium on the absorption edges (Fig. 2), the band gap energy of the anatase TiO_2 (Table 2) was found to be coherent with the variation in the c parameter of the anatase phase. In a recent paper [19], the band gap energy was related to the structural characteristic, demonstrating that, when the crystallinity of TiO_2 thin film is enhanced, the band gap energy shifts from 3.4 to 3.21 eV. In our work, the band gap energy calculated from the absorption edge was the highest at the lowest concentration of scandium, in accordance with the reduction of crystallinity observed in a comparison with the pure sample. However, with increasing scandium content, the band gap energy again decreased, despite the upper FWHM values, leading us to believe that the semiconductor characteristics were intrinsically changed by the insertion of scandium, owing to an enhancement of the quantum confinement effect.

The transmission spectra (Fig. 2) reveal a dislocation in the position of the fringes toward a higher wavelength as a function of the scandium amount. These effects of wave interference produced by the variation in film thickness were used to determine the thickness of the film through the fringe counting method. The thickness was calculated considering the number of fringes (N) generated at a continuous frequency sweep (Δv), refractive index (n) and light velocity (c), as described in Eq. 1:

$$\text{Thickness (nm)} = \frac{N}{2n} \cdot \frac{c}{\Delta v} \quad (1)$$

Thus, the calculated thicknesses of the films were 263, 276, 285, and 304 nm for TiO_2, $Sc_{0.005}Ti_{0.995}O_2$, $Sc_{0.02}Ti_{0.98}O_2$ and $Sc_{0.05}Ti_{0.95}O_2$ thin films, respectively, corresponding to an enhancement of 6 nm in thickness for each mol% of scandium, or 2 nm per mol% of scandium per number of dips. Figure 3 depicts a print screen of the FTG interface, showing the calculated thickness of the

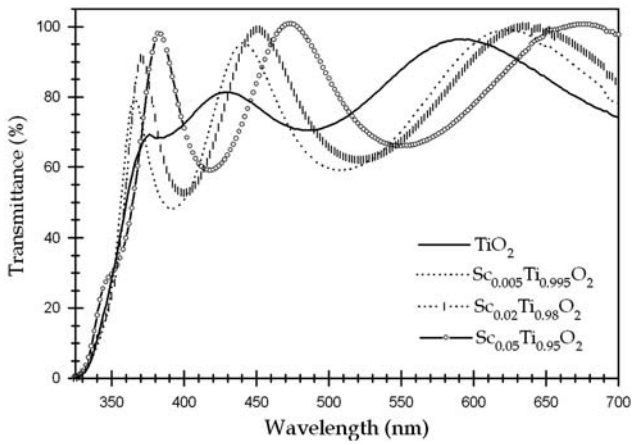

Fig. 2 Transmittance spectra for nondoped and Sc-doped TiO_2 thin films

Table 2 Optical parameters for the TiO_2 films obtained from Fig. 2

Sample	Absorption edge (nm)	Band gap energy (eV)
TiO_2	374	3.32
$Sc_{0.005}Ti_{0.995}O_2$	366	3.39
$Sc_{0.02}Ti_{0.98}O_2$	370	3.35
$Sc_{0.05}Ti_{0.95}O_2$	384	3.23

TiO_2 thin film and the low value of deviation, confirming the reliability of this software to calculate the thickness of thin films. Furthermore, to corroborate these data, the films thicknesses were visualized by scanning electron microscopy. The micrographs of all the fractured films showed that their thicknesses were very close to the calculated ones. To illustrate the congruity between the calculated and real thicknesses, Fig. 4a depicts a cross-section of the fractured TiO_2 thin film, which had a thickness of approximately 260 nm. In addition, the surface of the film depicted in the low magnification image (Fig. 4b) reveals good homogeneity, which is indicated by the formation of a small number of cracks.

The thin films were also investigated from a practical standpoint, studying their catalytic efficiency in the degradation of diclofenac potassium (DCFP) (Fig. 5). The photodegradation efficiency (Eff_P) was calculated by Eq. 2, where E is the real irradiance (W cm^{-2}) produced by a black-light incidence upon the thin film surface, V is the volume (L) of DCFP solution and A_{tf} is the surface area of the films (cm^2). These curves indicate that the quantity of Sc added was not directly related to the amount of organics degraded, since no direct correlation was found between the Eff_P and the scandium content. At low concentrations of scandium ($Sc_{0.005}Ti_{0.995}O_2$), the degradation process was slower than that of pure TiO_2, while the $Sc_{0.02}Ti_{0.98}O_2$ composition presented a behavior similar to that of the pure catalyst sample. On the other hand, the $Sc_{0.05}Ti_{0.95}O_2$ sample presented the highest photodegradation efficiency, reaching 4.5 mg C W^{-1} after 24 h. In fact, a direct relationship was found between band gap energy (Table 2) and photodegradation efficiency, i.e., the lower the band gap energy, the higher the catalyst photodegradation efficiency.

$$\mathrm{Eff_P} = \frac{(\mathrm{TOC_0} - \mathrm{TOC})\ V}{EA_{\mathrm{tf}}} \tag{2}$$

The reduction in the TOC values implies that a fraction of the organic material was decarboxylized, reducing the total organic carbon in the solution. The conversion of DCFP into 8-chlorocarbazole-1-acetic acid and of these two compounds into aliphatic structures does not obviously lead to a reduction of the total organic carbon. The decarboxylation of these substances requires the presence

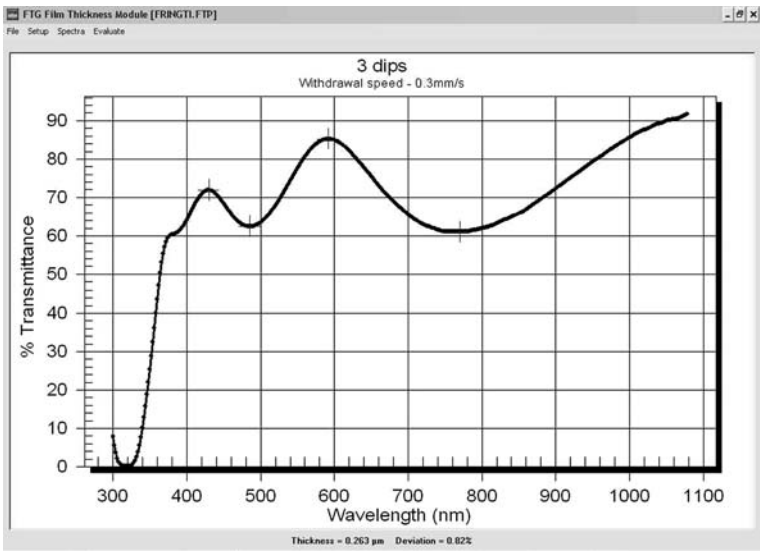

Fig. 3 Print screen of the FTG interface of the TiO_2 thin film coated three times

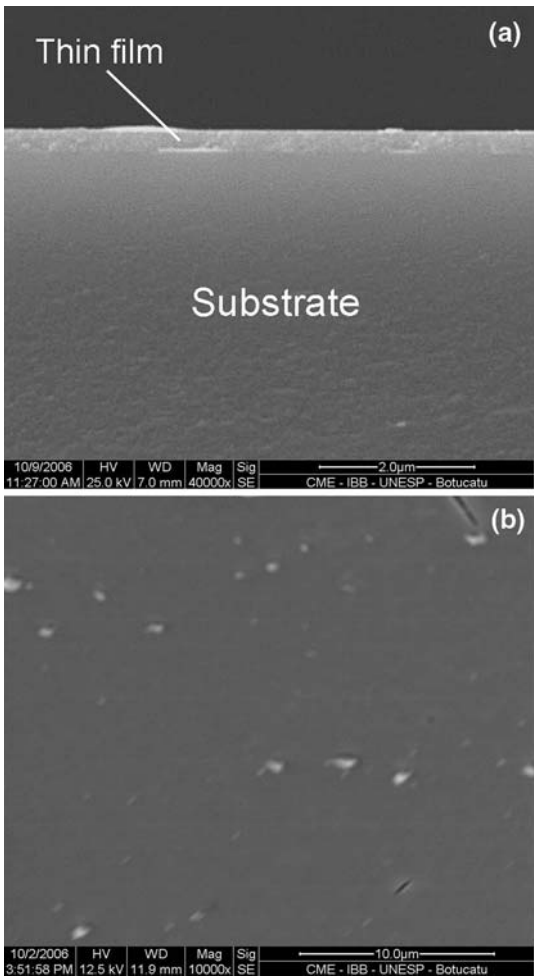

Fig. 4 Scanning electron micrographs of TiO_2 thin film: (**a**) high magnification of cross section and (**b**) low magnification of surface

of oxygen radicals, which require acidic conditions and oxygen dissolved in aqueous media [20]. Pure anatase TiO_2 contains equivalent populations of electrons and holes, but when donor dopants such as scandium are inserted into the semiconductor lattice, an excess of negative charge carriers is generated, enhancing the formation of oxygen radicals, thereby improving the oxidation processes. However, the insertion of scandium also increases the concentration of structural defects, which impair the film photoactivity due to the possible increase in the recombination of intrinsic excited electrons and holes by scattering. Thus, the photodegradation efficiency of these catalysts results from the competition between the population of negative charge carriers, which originate from the doping process, and the increased recombination caused by scattering, originated from the concentration of defects. Under the synthesis conditions employed here, a minimum of 2.0 mol% of scandium was necessary to increase the population of negative charge carriers to compensate for the scattering effects, while 5.0 mol% of Sc definitively improved the material's photoactivity.

The first derivative of the curves depicted in Fig. 5 is shown in Fig. 6. The resulting derivative ($dEff_P/dt$) can be interpreted as the photodegradation factor (mg C J^{-1}), which provides information about the optimal grade of light energy to degrade organic carbon in each stage of the process. The degradation process is divided into three distinct stages: the initial (up to 3 h), the intermediary (from 3 to 8 h) and the final stage (after 8 h). While the initial stage relates to the first decarboxylation of DCFP or 8-chlorocarbazole-1-acetic acid, its most probable photochemical derivative (Fig. 7), the final stage is associated with the mineralization of light organic compounds, which are generated in the intermediary process. The initial stage is the key to the degradation process because the catalysts

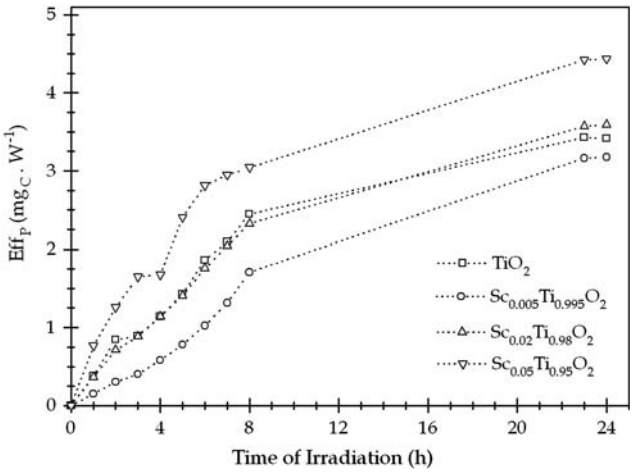

Fig. 5 Photodegradation efficiency of diclofenac potassium solution in the presence of Sc–TiO_2 catalysts

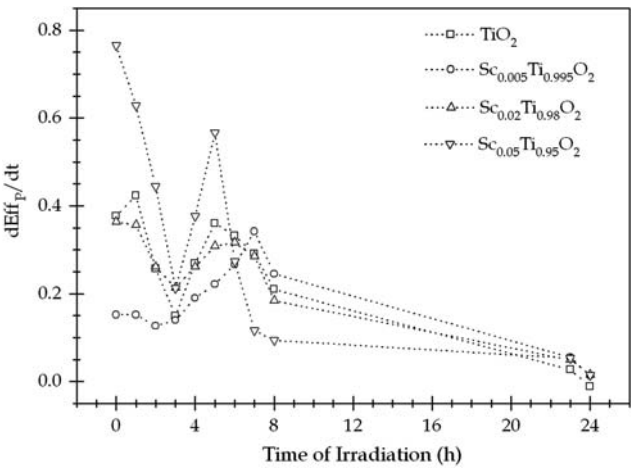

Fig. 6 Photodegradation factor of diclofenac potassium solution in the presence of Sc–TiO_2 catalysts

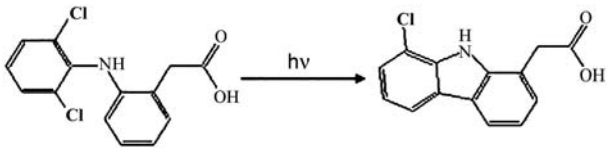

Fig. 7 Photochemical degradation of degraded diclofenac potassium into 8-chlorocarbazole-1-acetic acid

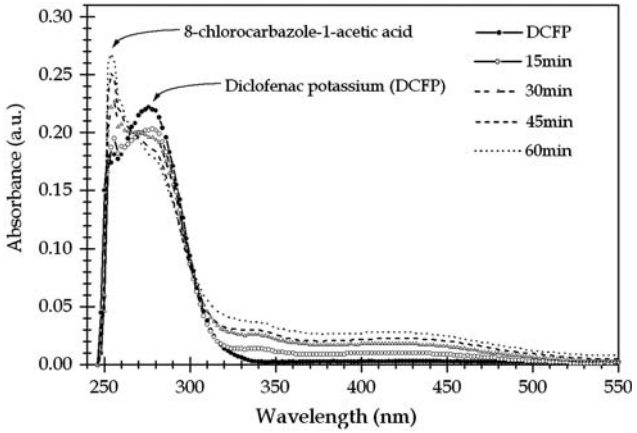

Fig. 8 Photochemical degradation of diclofenac potassium in the first hour of the process

that present the highest photodegradation factor in the initial stage also present a maximum photodegradation factor in the intermediary stage in a shorter period of time. Specifically, while the $Sc_{0.005}Ti_{0.995}O_2$ catalyst presented the maximum photodegradation factor at 7 h of degradation (Fig. 6) and a low value in the initial stage, the maximum photodegradation of the $Sc_{0.05}Ti_{0.95}O_2$ sample occurred in the intermediary stage (5 h) due to the high photodegradation factor in the initial stage.

The structures illustrated in Fig. 7 indicate that the aforementioned photochemical degradation involves a cyclization mechanism, and does not imply variations in the TOC values. For a detailed observation of the first hour of the degradation process without the catalyst, aliquots of the solution were collected at 15 min intervals. The curve profile in Fig. 8 shows that the photochemical degradation caused both a decrease in absorption at 276 nm and an increase in absorption at 252 nm. This was due to the fact that the black-light lamps used in the experiments emit radiation between 300 and 380 nm, causing overlapping with the DCFP absorption band. The correlation between each absorption band in the transmittance spectra and DCFP and 8-chlorocarbazole-1-acetic acid compounds was described by Koutsouba et al. [21].

Photodegradation was found to occur even when the solution was subjected to photocatalysis (not shown here), implying that the radiation (wavelength < 340 nm) incidence on the thin films was attenuated, since the films were immersed in the DCFP solution. Hence, the photoactivity of the thin films exhibiting lower absorption edges was impaired until significant amounts of DCFP were photodegraded. This fact was well illustrated by the $Sc_{0.005}Ti_{0.995}O_2$ sample, whose low absorption edge was associated to a low photodegradation factor.

Conclusions

The effects of scandium doping of anatase TiO_2 thin films revealed a direct correlation between structure and photocatalytic efficiency in the degradation of diclofenac potassium. The cell volume of the anatase TiO_2 phase was associated with variations in the absorption edge, and the insertion of 5.0 mol% of scandium into the anatase TiO_2 structure increased the absorption edge. A low concentration of scandium in the structure hindered the photoactivity due to the increase in structural defects, which reduced the cell volume. The modification in the absorption edge and the additional negative charge carriers generated by the doping process enhanced the photodegradation efficiency.

Acknowledgements The authors thank the Brazilian research-funding agency CAPES for the financial support.

References

1. Yates HM, Nolan MG, Sheel DW, Pemble ME (2006) J Photochem Photobiol A Chem 179:213
2. Keller V, Bernhardt P, Garin F (2003) J Catal 215:129
3. Choi H, Stathatos E, Dionysiou DD (2006) Appl Catal B Environ 63:60
4. Ternes T (1998) Water Res 32(11):3245
5. Quintero B, Miranda MA (2000) Ars Pharm 41(1):27
6. Suh HMS, Choi JR, Hah HJ, Koo SM, Bae YC (2004) J Photochem Photobiol A Chem 163:37
7. Yamaguchi F, Fujita T, Kanega Y, Ui K, Idemoto Y, Koura N (2004) Electrochemistry 72:156
8. Shchukin D, Ustinovich E, Sviridov D, Pichat P (2004) Photochem Photobiol Sci 3:142
9. Zang L, Lange C, Maier WF, Abraham I, Storck S, Kisch H (1998) J Phys Chem B 102:10765
10. Harada H, Hidaka H, Ueda T (1985) Res Bull Meisei Univ 21:45
11. Kisch H, Zang L, Lange C, Maier WF, Antonius C, Meissner D (1998) Angew Chem 110:3201
12. Chao HE, Yun YU, Xingfang HU, Larbot A (2003) J Eur Ceram Soc 23:14457
13. Moonsiri M, Rangsunvigit P, Chavade S, Gulari E (2004) Chem Eng J 97:241
14. Cannon AS, Morelli A, Pressler W, Warner JC, Guarrera D (2005) J Sol-Gel Sci Technol 36:157
15. Rietveld HM (1969) J Appl Cryst 10:65
16. Young RA, Wiles DB (1982) J Appl Cryst 15:430
17. Young RA, Larson AC, Paiva-Santos CO (1998) In: User's guide to program DBWS-9807 for Rietveld analysis of X-ray and

neutron powder diffraction patterns. School of Physics, Georgia Institute of Technology, Atlanta, GA
18. Shannon RD (1976) Acta Cryst A32:751
19. Guang-Lei T, Hong-Bo H, Jian-Da S (2005) Chinese Phys Lett 22:1787
20. Tanaka FS, Wien RG (1979) J Agric Food Chem 27(2):311
21. Koutsouba P, Dasenakis M, Hiskia A, Tsipi D (2001) In: Proceedings of the 7th international conference on environmental science and technology, Ermoupolis, Syros Island, Greece